https://doi.org/10.5194/egusphere-2026-7121
Preprint. Discussion started: 26 November 2026
© Author(s) 2026. CC BY 4.0 License.

Interactions between O_3 and $PM_{2.5}$ promote a regional double-high pollution event in the Yangtze River Delta, China

Xiaodong Xie[1], Yang Qin[2], Hongli Wang[3], Momei Qin[1], Yuanhang Zhang[4], Jianlin Hu[1,*]

[1]Jiangsu Key Laboratory of Intelligent Atmospheric Environment Monitoring and Carbon-Pollution Co-control, Collaborative Innovation Center of Atmospheric Environment and Equipment Technology, School of Environmental Science and Engineering, Nanjing University of Information Science and Technology, Nanjing 210044, China
[2]Henan Key Laboratory of Agrometeorological Support and Applied Technique, CMA, Henan Meteorological Observatory, Zhengzhou 450003, China
[3]State Environmental Protection Key Laboratory of Formation and Prevention of Urban Air Pollution Complex, Shanghai Academy of Environmental Sciences, Shanghai 200233, China
[4]State Key Joint Laboratory of Environmental Simulation and Pollution Control, College of Environmental Sciences and Engineering, Peking University, Beijing 100871, China

Correspondence to: Jianlin Hu (jianlinhu@nuist.edu.cn)

Abstract. $PM_{2.5}$ and O_3 typically peak in different seasons, yet co-occurrence of high $PM_{2.5}$ and high O_3 (double-high pollution, DHP) is frequently observed in China, and the coupling between the two pollutants remains unclear. Here, field observations and two-way coupled WRF-CMAQ simulations were used to investigate O_3-$PM_{2.5}$ interactions during a DHP event in the Yangtze River Delta (YRD) in April 2019. Nitrate dominated $PM_{2.5}$ in Shanghai and Nanjing on the DHP days, accounting for 31.7% and 41.3% of $PM_{2.5}$. High nighttime O_3 and strong oxidation capacity in the eastern YRD promoted nocturnal nitrate formation via N_2O_5 heterogeneous hydrolysis. Sensitivity simulations suggest that nighttime nitrate increased by 0.15 μg/m^3 per 1 μg/m^3 increase in O_3, approximately seven times the daytime response. Nighttime $PM_{2.5}$ transport and daytime photochemistry jointly drove DHP downwind, while aerosol radiative feedback further increased both pollutants. Our results highlight the critical roles of nighttime chemistry, regional transport, and aerosol–radiation feedback in DHP episodes, underscoring the need for coordinated O_3–$PM_{2.5}$ control in the YRD.

1. Introduction

Ground-level ozone (O_3) and fine particulate matter ($PM_{2.5}$) are the two primary air pollutants threatening public health and ecosystems (Fan et al., 2020; Wang et al., 2020). Exposure to high concentrations of O_3 and $PM_{2.5}$ increases morbidity and mortality through cardiovascular and respiratory diseases (Gao et al., 2017; Hu et al., 2017; Lefohn et al., 2018). Over the past decade, China has achieved remarkable improvements in ambient air quality, with the national average $PM_{2.5}$ concentration declining by approximately 42% from 2013 to 2022. Nevertheless, $PM_{2.5}$ levels in most urban areas remain 3 to over 10 times higher than the World Health Organization (WHO) guideline value (5 μg/m^3 annual mean), while O_3 concentrations have remained stubbornly high across most of China.[2] This dual challenge has underscored the urgent need for synergistic control strategies targeting both pollutants (He et al., 2024).

O_3 and $PM_{2.5}$ exhibit distinct seasonal patterns. O_3 concentrations usually peak in summer under intense photochemistry driven by strong solar radiation, whereas $PM_{2.5}$ pollution is normally severe in winter owing to enhanced residential heating emissions and stagnant meteorological conditions that trap pollutants near the surface (Wang et al., 2017). Despite this seasonal divergence, co-occurring high $PM_{2.5}$ and high O_3 pollution (double-high pollution, DHP), defined as days with

https://doi.org/10.5194/egusphere-2026-7121
Preprint. Discussion started: 26 November 2026
© Author(s) 2026. CC BY 4.0 License.

daily mean $PM_{2.5}$ ≥ 75 μg/m^3 and MDA8 O_3 ≥ 160 μg/m^3 (Grade II of the China National Ambient Air Quality Standard 2012), has been widely reported, and positive $PM_{2.5}$-O_3 correlations prevail over most of China (Zhu et al., 2019). In the United States, extreme heatwaves increased wildfire emissions and produced stagnant atmospheric circulation, causing widespread co-occurrence of high O_3 and $PM_{2.5}$ (Kalashnikov et al., 2022; Schnell and Prather, 2017). In China, DHP events have been documented in the Beijing-Tianjin-Hebei, the Yangtze River Delta (YRD), and the Pearl River Delta regions (Zong et al., 2021). A recent YRD study reported that 30 out of 413 polluted days in Shanghai during 2015–2019 were DHP days, occurring mostly in transitional seasons (April–May and September–October) (Qin et al., 2021).

The interaction between O_3 and $PM_{2.5}$ involves complex bidirectional feedbacks mediated by shared precursors, nitrogen oxides (NO_x) and volatile organic compounds (VOCs), as well as coupled atmospheric processes. O_3-derived radicals (e.g., OH and NO_3) can accelerate the oxidation of SO_2, NO_x, and VOCs to form secondary aerosols such as sulfate (SO_4^{2-}), nitrate (NO_3^-), and secondary organic aerosols (Wang et al., 2021; Zhao et al., 2020). In turn, $PM_{2.5}$ influences O_3 formation by scattering or absorbing solar radiation and by providing surfaces for the heterogeneous uptake of NO_2 and hydroperoxy (HO_2) radicals (Li et al., 2018). Such interactions presumably become more pronounced during DHP events. Most previous DHP studies, however, focused on long-term statistical patterns rather than the mechanisms of individual events, identifying weak synoptic circulation and regional transport of precursors as key drivers (Ma et al., 2023b; Zong et al., 2021). Few studies have quantified how O_3 regulates the burst growth of specific $PM_{2.5}$ components or how the radiative effect of $PM_{2.5}$ feeds back on O_3 during DHP events (Li et al., 2021). These limitations hinder the development of effective O_3-$PM_{2.5}$ synergistic control strategies (Kang et al., 2021).

This study addresses these limitations by focusing on a typical DHP episode that occurred in the YRD during 5–8 April 2019. Field observations and the online two-way coupled WRF-CMAQ model were used to unravel the mutual interactions between O_3 and $PM_{2.5}$ during this event. Specifically, we identified the key drivers of the burst growth of $PM_{2.5}$, quantified the impact of O_3 on the formation of NO_3^-, the dominant $PM_{2.5}$ component during the episode, and evaluated the influence of the $PM_{2.5}$ radiative effect on O_3 concentrations.

2. Methods

2.1 DHP episode and observation data

A severe regional DHP event occurred in the central and eastern YRD during 5–8 April 2019. As shown in Figure S2, Yancheng, Changzhou, and Shanghai first experienced DHP on 5–7 April, and large-scale DHP then developed in five other cities (Hangzhou, Shaoxing, Suzhou, Nanjing, and Chuzhou) on 8 April. During the event, the MDA8 O_3 and daily average $PM_{2.5}$ reached 183 and 83.25 μg/m^3, respectively, in Shanghai, and peaked at 195.6 and 80.3 μg/m^3, respectively, in Nanjing.

Hourly concentrations of air pollutants (e.g., $PM_{2.5}$, PM_{10}, O_3, NO_2, and SO_2) at the eight cities in the YRD were obtained from the China National Environmental Monitoring Center (https://air.cnemc.cn:18007/, last accessed on September 19, 2026) from 31 March to 10 April 2019. Hourly meteorological data (i.e., temperature, wind speed, wind direction, and relative humidity) were obtained from the China Meteorological Administration (http://data.cma.cn/en, last accessed on August 30, 2026). Ambient measurements of hourly water-soluble ions (SO_4^{2-}, NO_3^-, and ammonium) collected with a Gas Components and Aerosol Monitoring system (MARGA 1S), together with organic carbon (OC) and elemental carbon (EC), were conducted at two urban sites in Shanghai (31.2°N, 121.5°E) and Nanjing (32.1°N, 118.8°E). Detailed information on the observations is given in Section S3 of the Supporting Information (SI).

https://doi.org/10.5194/egusphere-2026-7121
Preprint. Discussion started: 26 November 2026
© Author(s) 2026. CC BY 4.0 License.

2.2 Model description and application

The two-way coupled Weather Research and Forecasting (WRF)-Community Multiscale Air Quality (CMAQ) model, version 5.2, was used in this study. Unlike the traditional offline CMAQ, the coupled model accounts for the effect of aerosol radiative feedback on meteorology and air quality (Grell and Baklanov, 2011; Wong et al., 2012), which is closer to the real atmosphere where aerosols and meteorology interact. A detailed description of the online two-way coupled WRF-CMAQ is given in Section S1 of the SI. Two nested domains with horizontal resolutions of 12 and 4 km (d01 and d02) are shown in Figure S1; d01 covers most of China and parts of East Asia, and d02 covers the entire YRD. The simulations were conducted from 25 March to 10 April 2019, with the first 6 days discarded as spin-up. The model configuration and emission inputs are described in Section S2 of the SI.

The process analysis (PA) methodology embedded in WRF-CMAQ was used to quantify the atmospheric processes governing simulated $PM_{2.5}$ and O_3. The integrated process rate (IPR) module tracked the hourly contributions of major processes to $PM_{2.5}$ and O_3, and integrated reaction rates (IRR) were used to evaluate the relative importance of gas-phase reactions in HNO_3 formation. Because of the large uncertainties in the aerosol indirect effect (Koch and Del Genio, 2010; Rosenfeld et al., 2019), only the aerosol direct effect was considered. Two scenarios were designed by switching the aerosol feedback option on and off: (1) YFb (with feedback) and (2) NoFb (no feedback). The aerosol direct effect was calculated as the difference between the two simulation results (YFb minus NoFb).

3. Results

3.1 The double high pollution episode

Figure 1 shows the variations of pollutants and meteorological conditions in Shanghai and Nanjing from 31 March to 9 April. High O_3 concentrations are often accompanied by higher temperature and intense photochemistry (Pu et al., 2017; Wang et al., 2017). Temperatures in Shanghai and Nanjing began to rise on 5 April, reaching maxima of 30.0 and 30.2 °C, respectively, at 14:00 on their respective DHP days (7 and 8 April), when the hourly maximum O_3 concentrations reached 203 and 225 μg/m^3, respectively. On 5 April, the MDA8 O_3 in Shanghai was 170 μg/m^3, exceeding the Grade II national standard (160 μg/m^3); the hourly maximum O_3 was 191 μg/m^3, the daily average $PM_{2.5}$ was 65.6 μg/m^3, and the maximum hourly $PM_{2.5}$ reached 82 μg/m^3. The average wind speed in Shanghai during 5–6 April was 2.1 m/s, and the warming and weak winds favored the transformation and accumulation of secondary pollutants. The DHP episodes in Shanghai and Nanjing on 7–8 April were simultaneously influenced by easterly transport, with the prevailing easterly winds carrying pollutants from the eastern YRD (Shanghai) to the western YRD (Nanjing). From 17:00 to 21:00 on 7 April, the average wind speed in Shanghai was 3.9 m/s while $PM_{2.5}$ increased explosively from 40 μg/m^3 at 17:00 to 151 μg/m^3 at 21:00. The increase in Nanjing was slower but persistent: $PM_{2.5}$ rose from 42 μg/m^3 at 17:00 on 7 April to a maximum of 110 μg/m^3 at 09:00 on 8 April, with an average wind speed of 4.0 m/s over this period. Near-surface O_3 is generally depleted at night by NO titration and dry deposition (Sillman, 1999; Xie et al., 2016), and typically declines until sunrise. In Nanjing, however, near-surface O_3 increased slightly from 35 μg/m^3 at 01:00 to 55 μg/m^3 at 06:00 before sunrise on 8 April. Considering the nighttime wind direction, this increase can reasonably be attributed to horizontal transport from the upstream area, which also preconditioned the high O_3 concentrations after sunrise.

NO_3^- was the most abundant component of $PM_{2.5}$ in both cities during the observation period (Figure 1). From 5 to 8 April, the average NO_3^- concentrations in Shanghai and Nanjing were 23.07 and 20.18 μg/m^3, accounting for 32.1% and 34.4% of $PM_{2.5}$, respectively, higher than the 15–25% typical of eastern China (Zhai et al., 2021) and comparable to winter haze levels in the YRD (Zang et al., 2022). On the respective DHP days the average NO_3^- concentrations were 26.38 and 33.17 μg/m^3, i.e., 31.7% and 41.3% of $PM_{2.5}$, exceeding the 5–8 April averages of the two cities. The high NO_3^- loading pushed

https://doi.org/10.5194/egusphere-2026-7121
Preprint. Discussion started: 26 November 2026
© Author(s) 2026. CC BY 4.0 License.

up the $PM_{2.5}$ concentration and was an important cause of the $PM_{2.5}$ exceedance on the DHP days. Sun et al. (2012) and Zhao et al. (2020) reported that high daytime temperature promotes NO_3^- decomposition, so NO_3^- accumulates mainly at night (Figure 1). On the night (19:00 to 06:00 the following morning) of 7 April, $PM_{2.5}$ increased rapidly, and the nighttime NO_3^- in both cities reached their highest values (44.75 and 41.80 μg/m³), accounting for 36.7% and 46.1% of nighttime $PM_{2.5}$, indicating that NO_3^- growth drove the nighttime $PM_{2.5}$ growth. The nitrogen oxidation ratio (NOR = $[NO_3^-]/([NO_3^-]+[NO_2])$, where the brackets denote molar concentrations) reflects the extent of secondary conversion of NO_2. The nighttime NOR values on 7 April were 0.35 and 0.38 in the two cities, higher than on any other night, confirming more extensive secondary inorganic aerosol formation.

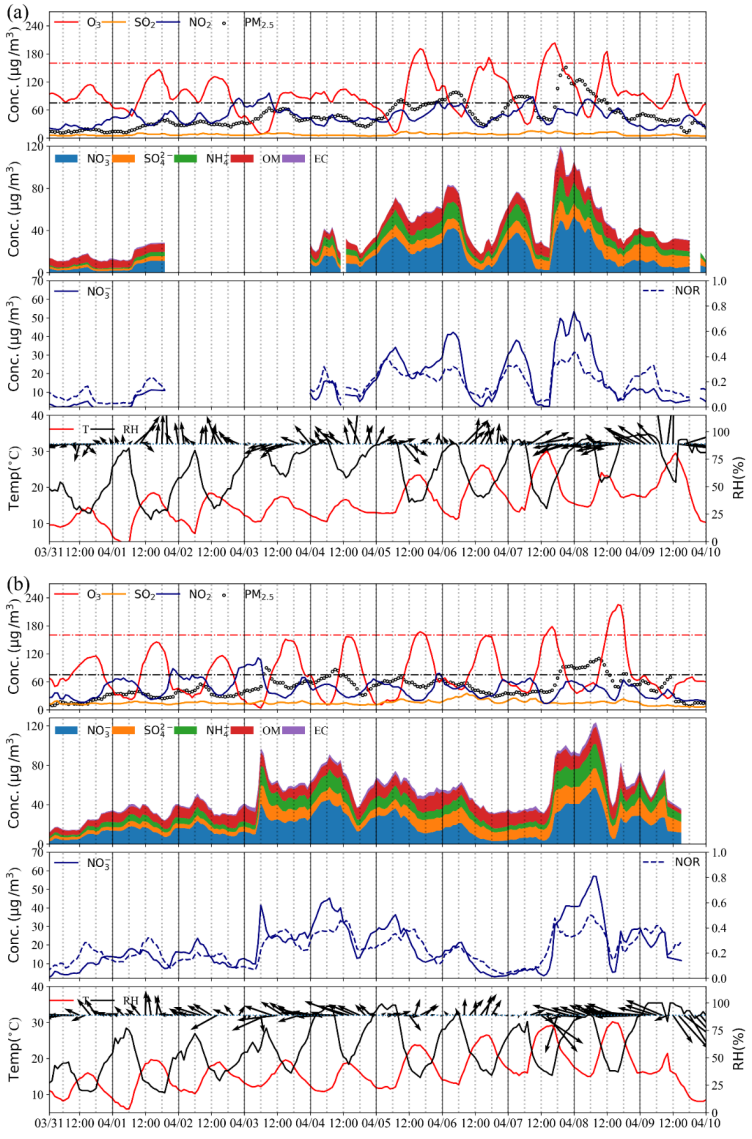


Figure 1. Time series of temperature (Temp), wind, relative humidity (RH), O_3, $PM_{2.5}$ and their chemical components in (a) Shanghai and (b) Nanjing during the study period

https://doi.org/10.5194/egusphere-2026-7121
Preprint. Discussion started: 26 November 2026
© Author(s) 2026. CC BY 4.0 License.

3.2 Process analysis of $PM_{2.5}$ and O_3

The coupled WRF-CMAQ was used to investigate the main driving processes and factors for the high $PM_{2.5}$ and O_3 in this episode. The model was evaluated at the eight cities that experienced DHP (Shanghai, Nanjing, Changzhou, Suzhou, Yancheng, Chuzhou, Hangzhou, and Shaoxing). A detailed model evaluation is given in Section S4 of the SI. In general, the coupled WRF-CMAQ reproduced the observed meteorological parameters and air pollutant concentrations reasonably well in most cities.

Driven by both local production and regional transport, high concentrations of $PM_{2.5}$ and O_3 accumulated over the eastern coastal YRD on the afternoon of 7 April (Figures S8 and S9). The lower-tropospheric winds at night were predominantly easterly, and an obvious transport of $PM_{2.5}$ and O_3 from the eastern YRD (Shanghai) to the western YRD (Nanjing) occurred along the upwind–downwind axis. Under these easterlies, $PM_{2.5}$ was transported mainly within the near-surface planetary boundary layer (PBL), whereas O_3 was transported mainly in the residual layer (Figure S14). Along the regional transport pathway (black line in Figure S1), the mean wind directions at the surface, 500 m, and 900 m were 90.2°, 143.9°, and 173.1° during 00:00–07:00 on 8 April (Figure S14), respectively. Owing to this directional shear, O_3 in the residual layer was transported gradually from westward to northward with height, and the O_3 concentration along the route decreased with height and time (Figure S12). The hourly average contribution of vertical mixing within the PBL during 08:00–10:00 on 8 April was 21.5 μg/m^3 along the Shanghai–Nanjing pathway (red line in Figure S1) and 17.3 μg/m^3 in the downwind Nanjing area (Figures S15a and S16d), the lowest values on 5–8 April. In contrast, the positive contributions of daytime photochemistry on 8 April reached 168.3 and 187.8 μg/m^3, far exceeding those on the previous three days. Strong photochemistry on 8 April was therefore the main cause of the O_3 pollution in the downwind area. Additional discussion is provided in Section S5 of the SI.

Process analysis of $PM_{2.5}$ and O_3 in the PBL was conducted for the two key cities along the transport pathway, Shanghai and Nanjing. The $PM_{2.5}$ aerosol process (AERO) in both cities was concentrated at night, and the AERO in Shanghai on 5–8 April was much higher than that in Nanjing (Figure S16). Both the O_3 photochemical (CHEM) process and $PM_{2.5}$ AERO from local production in Shanghai exceeded those in Nanjing, supplying substantial $PM_{2.5}$ and O_3 to the eastern YRD. A detailed discussion of IPR in the two cities is given in Section S6 of the SI.

High O_3 pollution occurred in the daytime, whereas $PM_{2.5}$ in both cities grew rapidly during the night of 7 April (Figure 1). We defined 17:00–22:00 on 7 April as the Shanghai $PM_{2.5}$ growth stage and 17:00 on 7 April to 09:00 on 8 April as the Nanjing $PM_{2.5}$ growth stage. The contributions of atmospheric processes to $PM_{2.5}$ and O_3 were calculated as:

$$Source_p = \frac{\sum_t IPR_{p,t}}{\sum_p \sum_t IPR_{p,t}} \times 100\% \quad (IPR_{p,t} > 0) \tag{1}$$

$$Sink_p = \frac{\sum_t IPR_{p,t}}{\sum_p \sum_t IPR_{p,t}} \times 100\% \quad (IPR_{p,t} < 0) \tag{2}$$

where p denotes an atmospheric process, t denotes time, and $Source_p$ and $Sink_p$ denote the positive and negative contributions of process p to $PM_{2.5}$ or O_3, respectively. A positive contribution indicates that the process acts as a source that increases the concentration, whereas a negative contribution indicates a sink that decreases the concentration.

The total positive contributions to O_3 in Shanghai and Nanjing were 253.1 and 313.1 μg/m^3, respectively, on their DHP days, with the larger value in Nanjing (Figure 2a-b). Vertical mixing was the dominant positive contributor in Shanghai (53.6%), whereas O_3 in Nanjing was generated mainly by local photochemistry (57.2%). Figure 2c-d shows the sources and sinks during the $PM_{2.5}$ growth stages. The average hourly production of $PM_{2.5}$ in Shanghai and Nanjing was 30.1 and

https://doi.org/10.5194/egusphere-2026-7121
Preprint. Discussion started: 26 November 2026
© Author(s) 2026. CC BY 4.0 License.

11.9 μg/m^3, and the average hourly removal was 14.3 and 7.0 μg/m^3, giving net hourly increases of 15.8 and 4.9 μg/m^3; hence the explosive rather than gradual increase in Shanghai. During the Shanghai growth stage, horizontal transport (HTRA) was the largest positive contributor (50.1%). In Nanjing, HTRA contributed 43.3%, slightly weaker than in Shanghai because of the local AERO production; AERO and HTRA contributed comparable shares (45.3% and 43.3%). In particular, during the second half of the Nanjing growth stage (04:00–09:00 on 8 April), HTRA significantly exceeded local production (Figure S16b). These results indicate that nighttime horizontal transport within the PBL was an important driver of $PM_{2.5}$ pollution on the DHP days in both cities.

NO_3^- was the major secondary inorganic ion in both cities (Figure 1). Figure 2e shows the composition of the NO_3^- sources during the growth stages. The hourly positive NO_3^- increments were 11.5 and 5.2 μg/m^3 in Shanghai and Nanjing, respectively. AERO and HTRA were the main NO_3^- sources in both cities: AERO contributed 63.9% in Nanjing, the dominant source of the Nanjing growth stage; and although the AERO share in Shanghai (42.4%) was lower, it remained the largest single contributor. Thus, although horizontal transport strongly affected the NO_3^- increase, the NO_3^- accumulating during the growth stages was produced mainly by local chemistry.

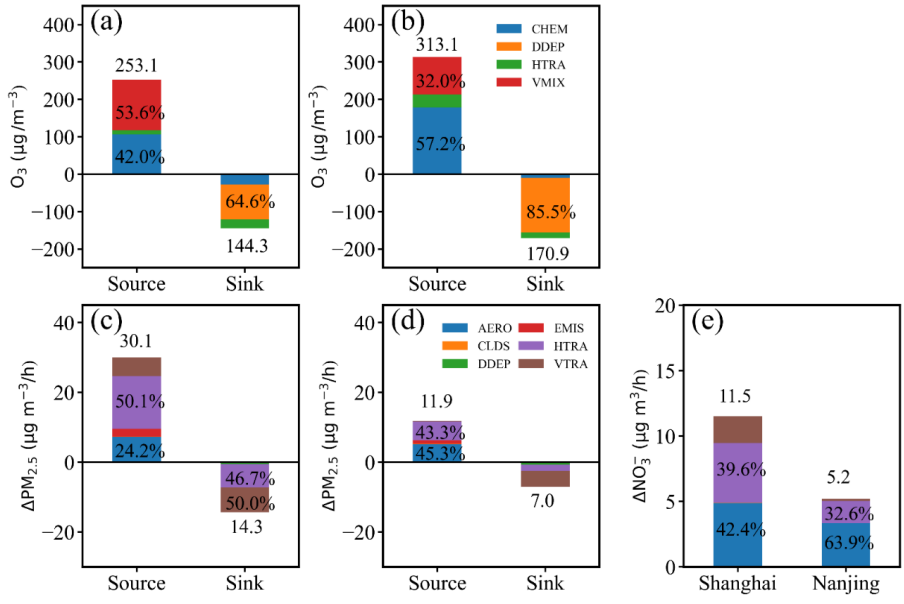


Figure 2. Total contributions of O_3 source and sink within the daytime PBL on DHP days in Shanghai (a) and Nanjing (b). Total contributions of $PM_{2.5}$ source and sink during $PM_{2.5}$ growth phase in Shanghai (c) and Nanjing (d). (e) Total source contribution of NO_3^- during $PM_{2.5}$ growth phase in Shanghai and Nanjing. AERO, DDEP, HTRA, CLDS, EMIS, and VTRA mean aerosol process, dry deposition, horizontal transport, cloud process, emission process, and vertical transport process. CHEM, DDEP, HTRA and VMIX mean photochemical process, dry deposition, horizontal transport, and vertical mixing.

3.3 The effect of O_3 on nitrate

O_3 pollution occurred mainly in the eastern YRD; we take Shanghai as an example to investigate the effect of O_3 on NO_3^-. The IPRs of NO_3^- in Shanghai during the clean (19:00 on 2 April to 06:00 on 5 April) and polluted (19:00 on 5 April to 06:00 on 8 April) periods are shown in Figure 3. The contribution of the aerosol process to NO_3^- was significantly higher on the polluted days than on the clean days. Because NO_3^- decomposes readily at high daytime temperatures, the nighttime change was emphasized. O_x (NO_2+O_3) was used to represent the atmospheric oxidation capacity. During the nighttime on

https://doi.org/10.5194/egusphere-2026-7121
Preprint. Discussion started: 26 November 2026
© Author(s) 2026. CC BY 4.0 License.

the polluted days, the average O_x, O_3, and the average NO_3^- production from the aerosol process in the PBL in Shanghai were 87.4 μg/m^3, 56.8 μg/m^3, and 6.1 μg/m^3/h, respectively, all higher than on the clean days (63.6 μg/m^3, 24.1 μg/m^3, and 3.0 μg/m^3/h) (Figure 3b-c). The nighttime average NO_2 concentration on the polluted days (30.6 μg/m^3) was lower than that on the clean days (39.5 μg/m^3). Figure S17 presents the NO_3^- production rates from different pathways. Generally, NO_3^- forms via two major pathways: the OH+NO_2 homogeneous reaction and the N_2O_5 heterogeneous reaction (Liu et al., 2020; Pathak et al., 2009). The first pathway occurs in the daytime, in which NO_2 reacts with OH to form gaseous HNO_3, which is subsequently neutralized by NH_3 to produce ammonium nitrate (NH_4NO_3) (Xie et al., 2022). The second pathway occurs mainly at night, in which the NO_3 radical, formed by the reaction of NO_2 with O_3, further reacts with NO_2 to establish a chemical equilibrium with dinitrogen pentoxide (N_2O_5), which then undergoes heterogeneous hydrolysis on wet particles (Chen et al., 2020; Fu et al., 2020). The percentage and yield of nitric acid from the heterogeneous reaction of N_2O_5 increased significantly from 5 April. The average reaction rate and proportion of the heterogeneous pathway on 2–4 April were 0.35 ppb/h and 51.2%, respectively, and those on 5–7 April were 0.72 ppb/h and 62.7%, respectively. This indicates that abundant NO_2 reacted with O_3 to generate NO_3 radicals during the polluted days, followed by the reaction with NO_2 to form N_2O_5 and subsequent heterogeneous conversion to NO_3^- at night. NO_2 was largely consumed during this period, leading to the lower NO_2 concentration than on the clean days. Therefore, under the strong atmospheric oxidation capacity, elevated O_3 promoted the chemical conversion of NO_2 to NO_3^-, increasing the secondary inorganic aerosol at night and ultimately driving the $PM_{2.5}$ exceedance.

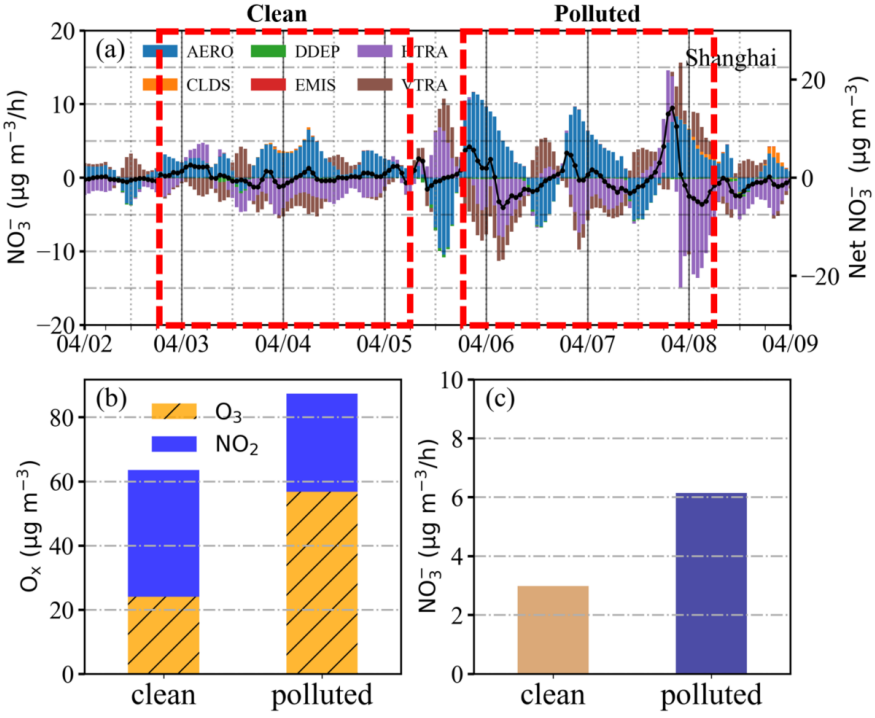


Figure 3. (a) Contributions of different processes to NO_3^- in the PBL over Shanghai (administrative region) on 2-9 April. The red boxes mark the clean (18:00 on 2 April to 06:00 on 5 April) and polluted (18:00 on 5 April to 06:00 on 8 April) periods. (b) Average nighttime (18:00-06:00) O_x (NO_2+O_3) concentrations in PBL over Shanghai during the clean and polluted periods. (c) Contributions of aerosol process to nighttime NO_3^- during the clean and polluted periods.

https://doi.org/10.5194/egusphere-2026-7121
Preprint. Discussion started: 26 November 2026
© Author(s) 2026. CC BY 4.0 License.

To isolate the impact of O_3 changes on surface NO_3^-, we further performed a sensitivity experiment in which the simulated O_3 concentrations entering the reactions of NO_2, OH, NO_3, N_2O_5, and HNO_3 were reduced by 20% during 5–8 April. Reducing O_3 in the chemistry module lowered the NO_3^- concentration (Figure 4), with the largest reductions at night (Figure 4c), and high NO_3^- reductions occurred in the central coastal areas of Jiangsu near Shanghai. The mean, daytime, and nighttime NO_3^- reductions in Shanghai were 1.55, 0.68, and 2.61 μg/m^3, respectively. We used $K = \Delta[NO_3^-]/\Delta[O_3]$ to measure the sensitivity of NO_3^- to O_3 changes. The regional distribution of K resembles that of the NO_3^- variation (Figure 4a-c); the response is strongest in the coastal areas of central Jiangsu, and K peaks at night. The average change rate (K_m) in Shanghai was about 0.07, the daytime rate (K_{dt}) about 0.02, and the nighttime rate (K_{nt}) about 0.15. This demonstrates that nighttime O_3 exerts a much stronger effect on NO_3^-: when the nighttime O_3 concentration in Shanghai decreases (increases) by 1 μg/m^3, the NO_3^- concentration decreases (increases) by approximately 0.15 μg/m^3.

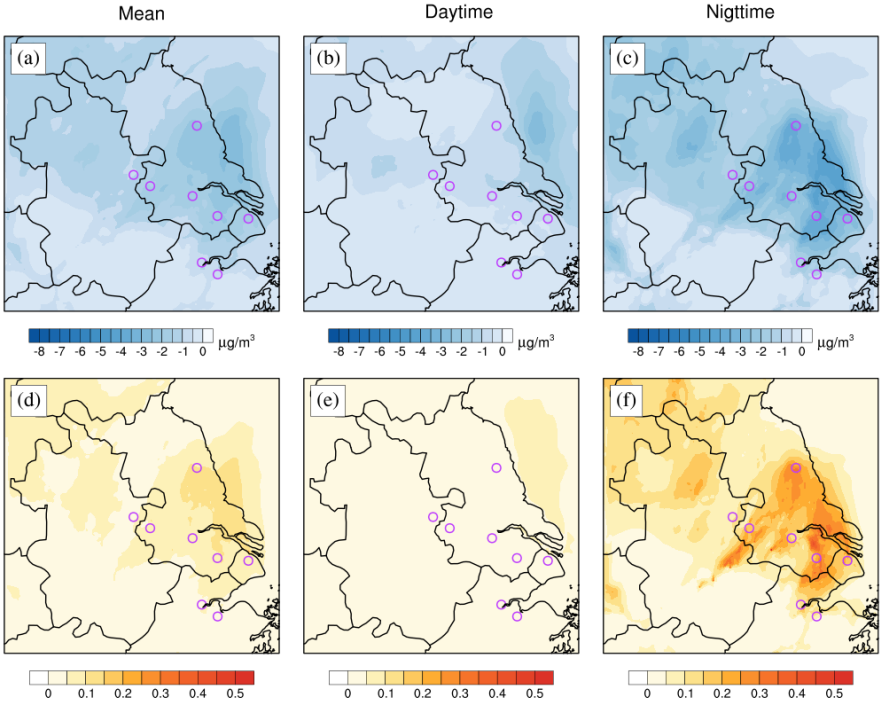


Figure 4. Responses of (a) mean, (b) daytime, and (c) nighttime NO_3^- to a 20% O_3 reduction on 5-8 April. The (d) mean (Km), (e) daytime (Kdt), and (f) nighttime (Knt) sensitivity of NO_3^- to O_3 changes.

3.4 Influence of the aerosol direct radiative effect on O_3 and $PM_{2.5}$

We further investigated the aerosol direct radiative effect (ADRE) on near-ground $PM_{2.5}$ and O_3 concentrations in the eight cities affected by DHP on their respective DHP days (Table S3). For $PM_{2.5}$, the ADRE increased the concentration in the seven cities other than Hangzhou, with the largest increases in Nanjing and Chuzhou (8.4 and 10.9 μg/m^3, respectively). The ADRE increased the 8-city average daily $PM_{2.5}$ by 4.3 μg/m^3 (5.4%), smaller than the $PM_{2.5}$ response to radiative feedback reported for winter haze episodes in China (Table S4) (Wang et al., 2022; Zhang et al., 2021). This difference arises because those studies focused on winter when particulate pollution is severe, whereas the present episode occurred in April with a lower aerosol loading.

https://doi.org/10.5194/egusphere-2026-7121
Preprint. Discussion started: 26 November 2026
© Author(s) 2026. CC BY 4.0 License.

In contrast to the O_3 decrease over the entire YRD during the whole pollution period (5–8 April) described in Section S7 of the SI, on the DHP days the average O_3 concentration in half of the DHP cities (Suzhou, Nanjing, Chuzhou, and Shaoxing) increased under the ADRE. Chuzhou and Shaoxing showed the largest increases (6.4 and 4.2 μg/m^3, respectively). As for MDA8 O_3, except for the decrease in Yancheng and the negligible change in Shanghai, it increased in the other six cities, with the largest increases in Chuzhou and Changzhou (21.1 and 13.0 μg/m^3, respectively). The ADRE increased the MDA8 O_3 by 6.9 μg/m^3 on average across the eight DHP cities. This implies that the ADRE increased daytime O_3 (Figure 5) and, to a certain extent, offset the O_3 reductions caused by the attenuation of photolysis rates (Dickerson et al., 1997) and the heterogeneous loss of oxidants on particles (Lou et al., 2014).

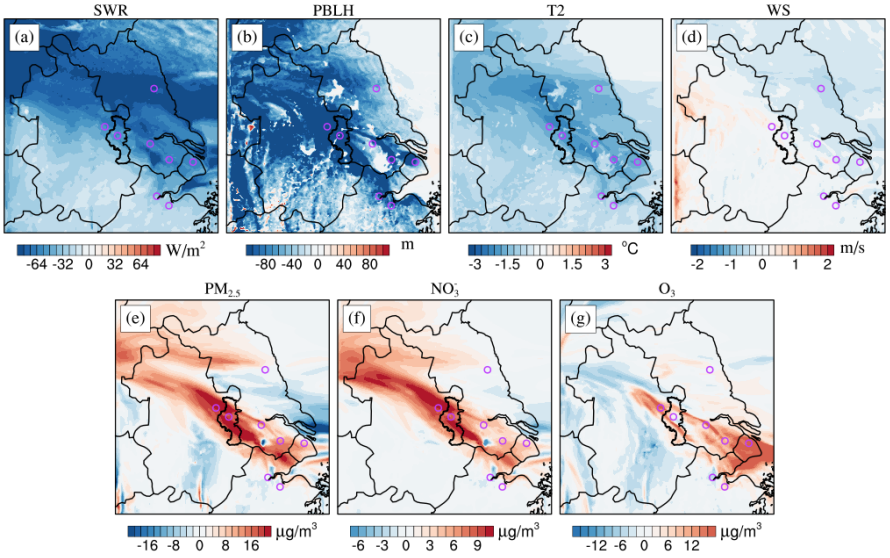


Figure 5. Responses of (a) SWR, (b) PBLH, (c) T2, (d) WS, (e) $PM_{2.5}$, (f) NO_3, and (g) O_3 to the ADRE (YFb-NoFb) during the daytime on 8 April.

Table S5 shows the influence of the ADRE on the physical and chemical processes affecting O_3 in the PBL of the eight DHP cities on their DHP days. Vertical mixing and photochemistry were the two processes with the largest increases induced by the aerosol radiative effect: vertical mixing increased by 23.4 μg/m^3 on average, the largest contribution, and photochemistry increased by 14 μg/m^3 on average. The ADRE thus enhanced both vertical mixing and photochemistry in the PBL, raising O_3 concentrations within and near the surface. Although most studies have emphasized the suppression of O_3 by aerosol attenuation of the actinic flux (Dickerson et al., 1997; Wang et al., 2019), recent modeling studies have shown that aerosol–radiation interactions can also enhance near-surface O_3 through altered atmospheric dynamics and vertical exchange (Qu et al., 2021; Yang et al., 2022). Vertical mixing and photochemistry were likewise the two processes driving the O_3 increase in this DHP event.

We take the Nanjing area as an example to investigate the reasons for the O_3 rise. Figure S19 shows the changes in the contributions of the physical and chemical processes affecting O_3 on the DHP day (8 April) in Nanjing under the NoFb scenario, including hourly O_3 averaged over the PBL, hourly O_3 near the surface, and daytime mean O_3 at different vertical layers. During the daytime, O_3 in the PBL was generated mainly by local photochemistry, the dominant source in the PBL (Figure S19a), whereas near-surface O_3 originated mainly from vertical mixing (Figure S19b). The average PBL height during the daytime on the DHP days in Nanjing was about 657 m (Figure S19c). Photochemistry was concentrated within

https://doi.org/10.5194/egusphere-2026-7121
Preprint. Discussion started: 26 November 2026
© Author(s) 2026. CC BY 4.0 License.

the PBL, and vertical mixing was positive near the surface and negative above it but below the PBL top, indicating that O_3 generated within the PBL was transported downward to the surface.

Figure 6a shows that the near-ground O_3 concentrations in the two scenarios differ little from 08:00 to 11:00, and the concentration in YFb is even slightly lower than that in NoFb. Starting at noon, the O_3 concentration in YFb increased markedly, and the ADRE on near-ground O_3 emerged. Compared with NoFb, the average O_3 concentration in YFb increased by 11.2 μg/m^3 during 12:00–18:00, with a maximum difference of 17.1 μg/m^3 at 16:00. Figures 6b and 6c show the changes in the physical and chemical contributions within the PBL and near the surface in Nanjing under the ADRE, respectively. The near-ground O_3 increase came mainly from vertical mixing, especially after 12:00, when the significant enhancement of vertical mixing raised the near-ground O_3. The O_3 increase in the vertical direction occurred mainly within the PBL (Figure 6d), and the ADRE significantly enhanced photochemistry within the PBL and vertical mixing near the surface (Figure 6e), which was the main reason for the near-ground O_3 rise. Therefore, the ADRE first enhanced photochemistry within the PBL and promoted the O_3 increase at high altitude; after 12:00, the strengthened vertical mixing transported more O_3 downward, raising the near-ground concentration.

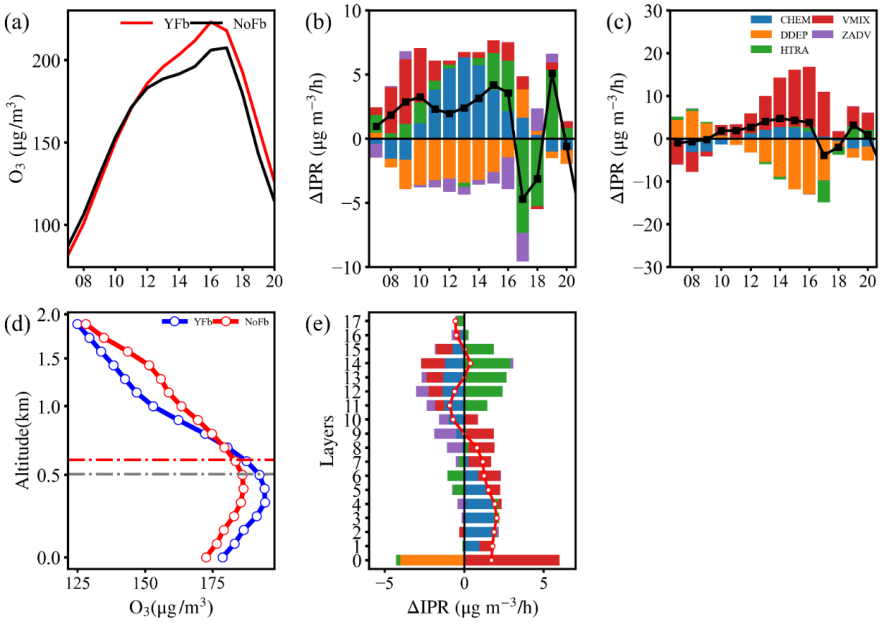


Figure 6. (a) Time series of ground O_3 concentrations under the YFb and NoFb scenarios on 8 April. Responses of atmospheric processes affecting O_3 to the ADRE in the PBL (b) and at the surface (c). (d) Vertical distribution of daytime O_3 concentrations under the YFb and NoFb scenarios. (e) Vertical distribution of the responses of atmospheric processes to the ADRE. The red and gray dashed lines in (d) denote the average daytime PBL heights under the YFb and NoFb scenarios, respectively.

4. Conclusions and Discussions

The nighttime N_2O_5 heterogeneous pathway identified here corroborates field and modeling evidence from northern China. The contribution of N_2O_5 hydrolysis to nocturnal NO_3^- production on the polluted days (62.7%) in this study is consistent with the 60–67% nocturnal share reported for O_3–$PM_{2.5}$ co-pollution episodes in the North China Plain (NCP) (Dai et al., 2024), the regime dependence of nocturnal NO_3^- formation via N_2O_5 hydrolysis (Ma et al., 2023a), and the dominance of the N_2O_5 pathway in intense NCP haze events (Chan et al., 2021). Direct measurements in Beijing likewise identify N_2O_5

https://doi.org/10.5194/egusphere-2026-7121
Preprint. Discussion started: 26 November 2026
© Author(s) 2026. CC BY 4.0 License.

and $ClNO_2$ as important nocturnal NO_3^- precursors (Zhou et al., 2025). Our results extend this mechanism to a spring DHP episode in the YRD, in which elevated nighttime O_3 sustained NO_3 production, in line with the finding that surface O_3 increases have driven NO_3^- deterioration in winter (Zhang et al., 2024) and with the heavy winter NO_3^- pollution attributed to enhanced photochemical oxidants in northern China (Fu et al., 2020). The sensitivity coefficient derived here ($K_{nt} \approx 0.15$) provides, to our knowledge, the first quantitative estimate of the O_3-to-NO_3^- coupling strength during a DHP event, complementing recent budget analyses of atmospheric oxidizing capacity in the YRD (Qin et al., 2022).

These results refine the mechanistic understanding of DHP development in transitional seasons. First, the episode was maintained by a relay between upwind nighttime oxidation and downwind daytime photochemistry: nocturnal O_3 surviving above the titration layer fueled N_2O_5 hydrolysis and NO_3^- accumulation upwind, and the NO_3^--rich aerosol was then transported downwind while residual-layer O_3 preconditioned the next day's photochemistry. Second, the $PM_{2.5}$-O_3 coupling during DHP is essentially a coupling through atmospheric oxidation capacity: O_3 promotes NO_3^- formation, the NO_3^--laden aerosol strengthens its own radiative feedback, and the feedback in turn enhances photochemistry and vertical mixing that feed O_3. This positive loop helps explain why MDA8 O_3 during DHP can exceed that during O_3-only pollution (Qin et al., 2021) and why $PM_{2.5}$ and O_3 are positively correlated under high-oxidation conditions (Qin et al., 2022). The spatial pattern of this synergic pollution in the YRD, concentrated along the Yangtze River and in transitional seasons (Zhu et al., 2023), is fully consistent with the episode analyzed here. Third, in contrast to the O_3 suppression commonly reported for winter haze (Dickerson et al., 1997; Wang et al., 2019), the ADRE in this spring episode increased O_3 in half of the DHP cities. This positive response agrees with the observed positive aerosol-O_3 association in Shanghai under low-VOC conditions (Liu et al., 2019), with the statistically significant but spatially variable PM radiative effect on O_3 in northern China (Li et al., 2021), and with modeling studies showing that the sign and magnitude of the aerosol effect on O_3 depend on aerosol loading, episode type, and vertical structure (Qu et al., 2021; Xing et al., 2017; Yang et al., 2022; Zhang et al., 2021). Given that NO_3^- has become an increasingly important driver of $PM_{2.5}$ pollution as SO_2 control succeeds (Xie et al., 2022), the O_3-driven nocturnal NO_3^- channel identified here is likely to become more significant in future DHP events.

Several uncertainties should be acknowledged. First, this study analyzed a single DHP episode in spring 2019, so the quantitative conclusions (e.g., the K values and ADRE magnitudes) are episode-specific, although the identified mechanisms are supported by the multi-year DHP climatology of the YRD and the meteorological analysis of co-pollution over eastern China (Ma et al., 2023b; Qin et al., 2021). Also, the N_2O_5 uptake coefficient and related heterogeneous parameters were prescribed rather than constrained by simultaneous measurements of NO_3, N_2O_5, and $ClNO_2$, introducing uncertainty into the partitioning of NO_3^- formation pathways (Chan et al., 2021; Zhou et al., 2025). In addition, the aerosol indirect effect was excluded because of its large uncertainty (Koch and Del Genio, 2010; Rosenfeld et al., 2019), so the total aerosol feedback on DHP may be underestimated.

Our findings have direct implications for the coordinated control of $PM_{2.5}$ and O_3 in the YRD. Because nocturnal O_3 strongly regulates NO_3^- formation, control strategies should account for nighttime chemistry rather than focusing solely on daytime O_3; reducing nocturnal O_3 through coordinated NO_x and VOCs reductions would also curb NO_3^-. The K analysis implies that O_3 reductions yield the largest NO_3^- benefits in coastal Jiangsu and Shanghai, highlighting priority areas for joint control. The positive ADRE feedback indicates that $PM_{2.5}$-only reductions may initially increase O_3 by enhancing photolysis (Kang et al., 2021; Xing et al., 2017), reinforcing the need for simultaneous VOCs and NO_x reductions with appropriate ratios (Li et al., 2018). What's more important, the transport relay identified along the Shanghai–Nanjing corridor underscores the value of regionally coordinated rather than city-level emission controls, in line with recent assessments of global $PM_{2.5}$–O_3 compound pollution (He et al., 2024).

https://doi.org/10.5194/egusphere-2026-7121
Preprint. Discussion started: 26 November 2026
© Author(s) 2026. CC BY 4.0 License.

Code and data availability

The observation data used in this study are available from the China National Environmental Monitoring Center (https://air.cnemc.cn:18007/) and the China Meteorological Administration (http://data.cma.cn/en). Model outputs are available from the corresponding author upon reasonable request.

Author contributions

J.H. conceptualized the study and supervised the research. X.X. and Y.Q. performed the simulations and data analysis., Y.Z., M.Q., and H.W. contributed to result interpretation. X.X., Y.Q., and J.H. wrote the manuscript, and all authors commented on and approved the final version.

Competing interests

The authors declare that they have no conflict of interest.

Acknowledgements

We are grateful for the support from the National Key Research and Development Program of China, the National Natural Science Foundation of China, Anyang National Climate Observatory Fund, and the Qing Lan Project of Colleges and Universities in Jiangsu Province.

Financial support

This work was supported by the National Key Research and Development Program of China (2023YFC3706100), the National Natural Science Foundation of China (42277095, 42305193), Anyang National Climate Observatory Fund (AYNCOF202301), and the Qing Lan Project of Colleges and Universities in Jiangsu Province.

References

Chan, Y. C., Evans, M. J., He, P., Holmes, C. D., Jaeglé, L., Kasibhatla, P., Liu, X. Y., Sherwen, T., Thornton, J. A., Wang, X., Xie, Z., Zhai, S., and Alexander, B.: Heterogeneous Nitrate Production Mechanisms in Intense Haze Events in the North China Plain, Journal of Geophysical Research: Atmospheres, 126, e2021JD034688, 10.1029/2021jd034688, 2021.

Chen, X., Wang, H., Lu, K., Li, C., Zhai, T., Tan, Z., Ma, X., Yang, X., Liu, Y., Chen, S., Dong, H., Li, X., Wu, Z., Hu, M., Zeng, L., and Zhang, Y.: Field Determination of Nitrate Formation Pathway in Winter Beijing, Environmental Science & Technology, 54, 9243-9253, 10.1021/acs.est.0c00972, 2020.

Dai, W., Cheng, K., Huang, X., and Xie, M.: Modeling Analysis of Nocturnal Nitrate Formation Pathways during Co-Occurrence of Ozone and $PM_{2.5}$ Pollution in North China Plain, Atmosphere, 15, 1220, 10.3390/atmos15101220, 2024.

Dickerson, R. R., Kondragunta, S., Stenchikov, G., Civerolo, K. L., Doddridge, B. G., and Holben, B. N.: The Impact of Aerosols on Solar Ultraviolet Radiation and Photochemical Smog, Science, 278, 827-830, 10.1126/science.278.5339.827, 1997.

Fan, H., Zhao, C., and Yang, Y.: A comprehensive analysis of the spatio-temporal variation of urban air pollution in China

https://doi.org/10.5194/egusphere-2026-7121
Preprint. Discussion started: 26 November 2026
© Author(s) 2026. CC BY 4.0 License.

during 2014–2018, Atmospheric Environment, 220, 117066, 10.1016/j.atmosenv.2019.117066, 2020.

Fu, X., Wang, T., Gao, J., Wang, P., Liu, Y., Wang, S., Zhao, B., and Xue, L.: Persistent Heavy Winter Nitrate Pollution Driven by Increased Photochemical Oxidants in Northern China, Environmental Science & Technology, 54, 3881-3889, 10.1021/acs.est.9b07248, 2020.

Gao, J., Woodward, A., Vardoulakis, S., Kovats, S., Wilkinson, P., Li, L., Xu, L., Li, J., Yang, J., Li, J., Cao, L., Liu, X., Wu, H., and Liu, Q.: Haze, public health and mitigation measures in China: A review of the current evidence for further policy response, Science of The Total Environment, 578, 148-157, 10.1016/j.scitotenv.2016.10.231, 2017.

Grell, G. and Baklanov, A.: Integrated modeling for forecasting weather and air quality: A call for fully coupled approaches, Atmospheric Environment, 45, 6845-6851, 10.1016/j.atmosenv.2011.01.017, 2011.

He, C., Liu, J., Zhou, Y., Zhou, J., Zhang, L., Wang, Y., Liu, L., and Peng, S.: Synergistic $PM_{2.5}$ and O_3 control to address the emerging global $PM_{2.5}$-O_3 compound pollution challenges, Eco-Environment & Health, 3, 325-337, 10.1016/j.eehl.2024.04.004, 2024.

Hu, J., Huang, L., Chen, M., Liao, H., Zhang, H., Wang, S., Zhang, Q., and Ying, Q.: Premature Mortality Attributable to Particulate Matter in China: Source Contributions and Responses to Reductions, Environmental Science & Technology, 51, 9950-9959, 10.1021/acs.est.7b03193, 2017.

Kalashnikov, D. A., Schnell, J. L., Abatzoglou, J. T., Swain, D. L., and Singh, D.: Increasing co-occurrence of fine particulate matter and ground-level ozone extremes in the western United States, Science Advances, 8, eabi9386, 10.1126/sciadv.abi9386, 2022.

Kang, M., Zhang, J., Zhang, H., and Ying, Q.: On the Relevancy of Observed Ozone Increase during COVID-19 Lockdown to Summertime Ozone and $PM_{2.5}$ Control Policies in China, Environmental Science & Technology Letters, 8, 289-294, 10.1021/acs.estlett.1c00036, 2021.

Koch, D. and Del Genio, A. D.: Black carbon semi-direct effects on cloud cover: review and synthesis, Atmospheric Chemistry and Physics, 10, 7685-7696, 10.5194/acp-10-7685-2010, 2010.

Lefohn, A. S., Malley, C. S., Smith, L., Wells, B., Hazucha, M., Simon, H., Naik, V., Mills, G., Schultz, M. G., Paoletti, E., De Marco, A., Xu, X., Zhang, L., Wang, T., Neufeld, H. S., Musselman, R. C., Tarasick, D., Brauer, M., Feng, Z., Tang, H., Kobayashi, K., Sicard, P., Solberg, S., and Gerosa, G.: Tropospheric ozone assessment report: Global ozone metrics for climate change, human health, and crop/ecosystem research, Elementa: Science of the Anthropocene, 6, 28, 10.1525/elementa.279, 2018.

Li, K., Jacob, D. J., Liao, H., Shen, L., Zhang, Q., and Bates, K. H.: Anthropogenic drivers of 2013–2017 trends in summer surface ozone in China, Proceedings of the National Academy of Sciences, 116, 422-427, 10.1073/pnas.1812168116, 2018.

Li, S., Liu, R., Wang, S., and Chen, S. X.: Radiative Effects of Particular Matters on Ozone Pollution in Six North China Cities, Journal of Geophysical Research: Atmospheres, 126, e2020JD033419, 10.1029/2021jd035963, 2021.

Liu, L., Bei, N., Hu, B., Wu, J., Liu, S., Li, X., Wang, R., Liu, Z., Shen, Z., and Li, G.: Wintertime nitrate formation pathways in the north China plain: Importance of N_2O_5 heterogeneous hydrolysis, Environmental Pollution, 266, 115287, 10.1016/j.envpol.2020.115287, 2020.

Liu, Q., Liu, T., Chen, Y., Xu, J., Gao, W., Zhang, H., and Yao, Y.: Effects of aerosols on the surface ozone generation via a study of the interaction of ozone and its precursors during the summer in Shanghai, China, Science of The Total Environment, 675, 235-246, 10.1016/j.scitotenv.2019.04.121, 2019.

Lou, S., Liao, H., and Zhu, B.: Impacts of aerosols on surface-layer ozone concentrations in China through heterogeneous reactions and changes in photolysis rates, Atmospheric Environment, 85, 123-138, 10.1016/j.atmosenv.2013.12.004, 2014.

Ma, P., Quan, J., Dou, Y., Pan, Y., Liao, Z., Cheng, Z., Jia, X., Wang, Q., Zhan, J., Ma, W., Zheng, F., Wang, Y., Zhang, Y., Hua, C., Yan, C., Kulmala, M., Liu, Y., Huang, X., Yuan, B., Brown, S. S., and Liu, Y.: Regime-Dependence of

https://doi.org/10.5194/egusphere-2026-7121
Preprint. Discussion started: 26 November 2026
© Author(s) 2026. CC BY 4.0 License.



Nocturnal Nitrate Formation via N_2O_5 Hydrolysis and Its Implication for Mitigating Nitrate Pollution, Geophysical Research Letters, 50, e2023GL106183, 10.1029/2023gl106183, 2023a.

Ma, X., Yin, Z., Cao, B., and Wang, H.: Meteorological influences on co-occurrence of O_3 and $PM_{2.5}$ pollution and implication for emission reductions in Beijing-Tianjin-Hebei, Science China Earth Sciences, 66, 1258-1267, 10.1007/s11430-022-1070-y, 2023b.

Pathak, R. K., Wu, W. S., and Wang, T.: Summertime $PM_{2.5}$ ionic species in four major cities of China: nitrate formation in an ammonia-deficient atmosphere, Atmospheric Chemistry and Physics, 9, 1711-1722, 10.5194/acp-9-1711-2009, 2009.

Pu, X., Wang, T. J., Huang, X., Melas, D., Zanis, P., Papanastasiou, D. K., and Poupkou, A.: Enhanced surface ozone during the heat wave of 2013 in Yangtze River Delta region, China, Science of The Total Environment, 603-604, 807-816, 10.1016/j.scitotenv.2017.03.056, 2017.

Qin, M., Hu, A., Mao, J., Li, X., Sheng, L., Sun, J., Li, J., Wang, X., Zhang, Y., and Hu, J.: $PM_{2.5}$ and O_3 relationships affected by the atmospheric oxidizing capacity in the Yangtze River Delta, China, Science of The Total Environment, 810, 152268, 10.1016/j.scitotenv.2021.152268, 2022.

Qin, Y., Li, J., Gong, K., Wu, Z., Chen, M., Qin, M., Huang, L., and Hu, J.: Double high pollution events in the Yangtze River Delta from 2015 to 2019: Characteristics, trends, and meteorological situations, Science of The Total Environment, 792, 148349, 10.1016/j.scitotenv.2021.148349, 2021.

Qu, Y., Voulgarakis, A., Wang, T., Kasoar, M., Wells, C., Yuan, C., Varma, S., and Mansfield, L.: A study of the effect of aerosols on surface ozone through meteorology feedbacks over China, Atmospheric Chemistry and Physics, 21, 5705-5718, 10.5194/acp-21-5705-2021, 2021.

Rosenfeld, D., Zhu, Y., Wang, M., Zheng, Y., Goren, T., and Yu, S.: Aerosol-driven droplet concentrations dominate coverage and water of oceanic low-level clouds, Science, 363, eaav0566, 10.1126/science.aav0566, 2019.

Schnell, J. L. and Prather, M. J.: Co-occurrence of extremes in surface ozone, particulate matter, and temperature over eastern North America, Proceedings of the National Academy of Sciences, 114, 2854-2859, 10.1073/pnas.1614453114, 2017.

Sillman, S.: The relation between ozone, NO_x and hydrocarbons in urban and polluted rural environments, Atmospheric Environment, 33, 1821-1845, 10.1016/s1352-2310(98)00345-8, 1999.

Sun, Y., Wang, Z., Dong, H., Yang, T., Li, J., Pan, X., Chen, P., and Jayne, J. T.: Characterization of summer organic and inorganic aerosols in Beijing, China with an Aerosol Chemical Speciation Monitor, Atmospheric Environment, 51, 250-259, 10.1016/j.atmosenv.2012.01.013, 2012.

Wang, H., Lu, K., Chen, S., Li, X., Zeng, L., Hu, M., and Zhang, Y.: Characterizing nitrate radical budget trends in Beijing during 2013–2019, Science of The Total Environment, 795, 148869, 10.1016/j.scitotenv.2021.148869, 2021.

Wang, J., Xing, J., Wang, S., Mathur, R., Wang, J., Zhang, Y., Liu, C., Pleim, J., Ding, D., Chang, X., Jiang, J., Zhao, P., Sahu, S. K., Jin, Y., Wong, D. C., and Hao, J.: The pathway of impacts of aerosol direct effects on secondary inorganic aerosol formation, Atmospheric Chemistry and Physics, 22, 5147-5156, 10.5194/acp-22-5147-2022, 2022.

Wang, T., Xue, L., Brimblecombe, P., Lam, Y. F., Li, L., and Zhang, L.: Ozone pollution in China: A review of concentrations, meteorological influences, chemical precursors, and effects, Science of The Total Environment, 575, 1582-1596, 10.1016/j.scitotenv.2016.10.081, 2017.

Wang, W., Li, X., Shao, M., Hu, M., Zeng, L., Wu, Y., and Tan, T.: The impact of aerosols on photolysis frequencies and ozone production in Beijing during the 4-year period 2012–2015, Atmospheric Chemistry and Physics, 19, 9413-9429, 10.5194/acp-19-9413-2019, 2019.

Wang, Y., Gao, W., Wang, S., Song, T., Gong, Z., Ji, D., Wang, L., Liu, Z., Tang, G., Huo, Y., Tian, S., Li, J., Li, M., Yang, Y., Chu, B., Petäjä, T., Kerminen, V.-M., He, H., Hao, J., Kulmala, M., Wang, Y., and Zhang, Y.: Contrasting trends of $PM_{2.5}$ and surface-ozone concentrations in China from 2013 to 2017, National Science Review, 7, 1331-1339,

https://doi.org/10.5194/egusphere-2026-7121
Preprint. Discussion started: 26 November 2026
© Author(s) 2026. CC BY 4.0 License.



10.1093/nsr/nwaa032, 2020.

Wong, D. C., Pleim, J., Mathur, R., Binkowski, F., Otte, T., Gilliam, R., Pouliot, G., Xiu, A., Young, J. O., and Kang, D.: WRF-CMAQ two-way coupled system with aerosol feedback: software development and preliminary results, Geoscientific Model Development, 5, 299-312, 10.5194/gmd-5-299-2012, 2012.

Xie, M., Zhu, K., Wang, T., Chen, P., Han, Y., Li, S., Zhuang, B., and Shu, L.: Temporal characterization and regional contribution to O_3 and NO_x at an urban and a suburban site in Nanjing, China, Science of The Total Environment, 551-552, 533-545, 10.1016/j.scitotenv.2016.02.047, 2016.

Xie, X., Hu, J., Qin, M., Guo, S., Hu, M., Wang, H., Lou, S., Li, J., Sun, J., Li, X., Sheng, L., Zhu, J., Chen, G., Yin, J., Fu, W., Huang, C., and Zhang, Y.: Modeling particulate nitrate in China: Current findings and future directions, Environment International, 166, 107369, 10.1016/j.envint.2022.107369, 2022.

Xing, J., Wang, J., Mathur, R., Wang, S., Sarwar, G., Pleim, J., Hogrefe, C., Zhang, Y., Jiang, J., Wong, D. C., and Hao, J.: Impacts of aerosol direct effects on tropospheric ozone through changes in atmospheric dynamics and photolysis rates, Atmospheric Chemistry and Physics, 17, 9869-9883, 10.5194/acp-17-9869-2017, 2017.

Yang, H., Chen, L., Liao, H., Zhu, J., Wang, W., and Li, X.: Impacts of aerosol–photolysis interaction and aerosol–radiation feedback on surface-layer ozone in North China during multi-pollutant air pollution episodes, Atmospheric Chemistry and Physics, 22, 4101-4116, 10.5194/acp-22-4101-2022, 2022.

Zang, H., Zhao, Y., Huo, J., Zhao, Q., Fu, Q., Duan, Y., Shao, J., Huang, C., An, J., Xue, L., Li, Z., Li, C., and Xiao, H.: High atmospheric oxidation capacity drives wintertime nitrate pollution in the eastern Yangtze River Delta of China, Atmospheric Chemistry and Physics, 22, 4355-4374, 10.5194/acp-22-4355-2022, 2022.

Zhai, S., Jacob, D. J., Wang, X., Liu, Z., Wen, T., Shah, V., Li, K., Moch, J. M., Bates, K. H., Song, S., Shen, L., Zhang, Y., Luo, G., Yu, F., Sun, Y., Wang, L., Qi, M., Tao, J., Gui, K., Xu, H., Zhang, Q., Zhao, T., Wang, Y., Lee, H. C., Choi, H., and Liao, H.: Control of particulate nitrate air pollution in China, Nature Geoscience, 14, 389-395, 10.1038/s41561-021-00726-z, 2021.

Zhang, X., Yuan, C., and Zhuang, Z.: Exploring the Change in $PM_{2.5}$ and Ozone Concentrations Caused by Aerosol–Radiation Interactions and Aerosol–Cloud Interactions and the Relationship with Meteorological Factors, Atmosphere, 12, 1585, 10.3390/atmos12121585, 2021.

Zhang, Z., Lu, B., Liu, C., Meng, X., Jiang, J., Herrmann, H., Chen, J., and Li, X.: Nitrate pollution deterioration in winter driven by surface ozone increase, npj Climate and Atmospheric Science, 7, 160, 10.1038/s41612-024-00667-5, 2024.

Zhao, D., Liu, G., Xin, J., Quan, J., Wang, Y., Wang, X., Dai, L., Gao, W., Tang, G., Hu, B., Ma, Y., Wu, X., Wang, L., Liu, Z., and Wu, F.: Haze pollution under a high atmospheric oxidization capacity in summer in Beijing: insights into formation mechanism of atmospheric physicochemical processes, Atmospheric Chemistry and Physics, 20, 4575-4592, 10.5194/acp-20-4575-2020, 2020.

Zhou, W., Du, H., Liu, M., Xu, W., Zhao, J., Xie, C., Wang, Q., Zhang, Z., Zhang, Z., Li, J., Wang, W., Wang, Z., and Sun, Y.: Role of N_2O_5 heterogeneous hydrolysis in summer nitrate formation in Beijing: insights from direct measurements and model simulations, npj Clean Air, 1, 40, 10.1038/s44407-025-00039-0, 2025.

Zhu, J., Chen, L., Liao, H., and Dang, R.: Correlations between $PM_{2.5}$ and Ozone over China and Associated Underlying Reasons, Atmosphere, 10, 352, 10.3390/atmos10070352, 2019.

Zhu, Q., Yu, Y., Gong, H., Wang, Y., Wang, H., Wang, W., Xu, B., and Cheng, T.: Spatio-temporal characteristics of $PM_{2.5}$ and O_3 synergic pollutions and influence factors in the Yangtze River Delta, Frontiers in Environmental Science, 10, 1104013, 10.3389/fenvs.2022.1104013, 2023.

Zong, L., Yang, Y., Gao, M., Wang, H., Wang, P., Zhang, H., Wang, L., Ning, G., Liu, C., Li, Y., and Gao, Z.: Large-scale synoptic drivers of co-occurring summertime ozone and $PM_{2.5}$ pollution in eastern China, Atmospheric Chemistry and Physics, 21, 9105-9124, 10.5194/acp-21-9105-2021, 2021.